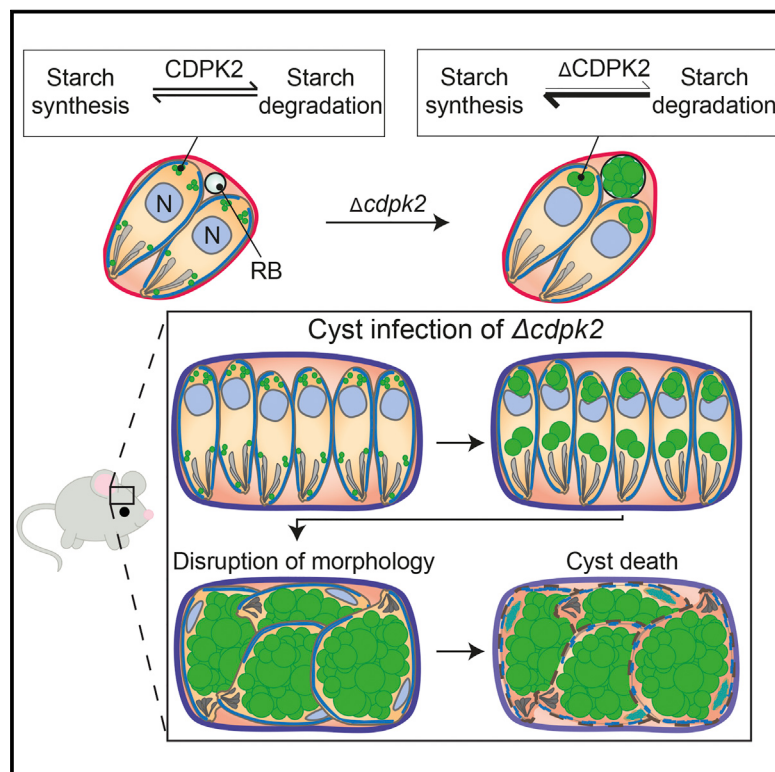


# Cell Host & Microbe

## Regulation of Starch Stores by a $\text{Ca}^{2+}$ -Dependent Protein Kinase Is Essential for Viable Cyst Development in *Toxoplasma gondii*

### Graphical Abstract



### Authors

Alessandro D. Ubaldi,  
James M. McCoy, Martin Blume, ...,  
Andrew I. Webb,  
Malcolm J. McConville,  
Christopher J. Tonkin

### Correspondence

[tonkin@wehi.edu.au](mailto:tonkin@wehi.edu.au)

### In Brief

Encysted lifecycle stages of *Toxoplasma gondii* produce and store starch. Ubaldi et al. show that the kinase CDPK2 is targeted to starch stores and regulates starch turnover in a  $\text{Ca}^{2+}$ -dependent manner. CDPK2 deficiency leads to unchecked starch accumulation and death of parasite tissue cysts.

### Highlights

- The *Toxoplasma* kinase CDPK2 has functional  $\text{Ca}^{2+}$ - and carbohydrate-binding domains
- CDPK2 deficiency causes unchecked accumulation of starch in *Toxoplasma* parasites
- Phosphorylation of several starch-metabolic enzymes relies on CDPK2 activity
- Loss of CDPK2 results in starch hyperaccumulation and death of chronic-stage parasites

# Regulation of Starch Stores by a $\text{Ca}^{2+}$ -Dependent Protein Kinase Is Essential for Viable Cyst Development in *Toxoplasma gondii*

Alessandro D. Ubaldi,<sup>1,2,7</sup> James M. McCoy,<sup>1,2,7</sup> Martin Blume,<sup>3</sup> Motti Gerlic,<sup>1,2</sup> David J.P. Ferguson,<sup>4</sup> Laura F. Dagley,<sup>1,2</sup> Cherie T. Beahan,<sup>5</sup> David I. Stapleton,<sup>6</sup> Paul R. Gooley,<sup>3</sup> Antony Bacic,<sup>5</sup> Seth L. Masters,<sup>1,2</sup> Andrew I. Webb,<sup>1,2</sup> Malcolm J. McConville,<sup>3</sup> and Christopher J. Tonkin<sup>1,2,\*</sup>

<sup>1</sup>The Walter and Eliza Hall Institute of Medical Research, 1G Royal Parade, Victoria, 3052, Australia

<sup>2</sup>Department of Medical Biology, The University of Melbourne, Victoria, 3010, Australia

<sup>3</sup>Department of Biochemistry and Molecular Biology, Bio21 Molecular Science & Biotechnology Institute, The University of Melbourne, Parkville, VIC, 3010, Australia

<sup>4</sup>Nuffield Department of Clinical Laboratory Science, Oxford University, John Radcliffe Hospital, Oxford OX3 9DU, United Kingdom

<sup>5</sup>ARC Centre of Excellence in Plant Cell Walls, The School of Botany, The University of Melbourne, Victoria, 3010, Australia

<sup>6</sup>The Department of Physiology, The University of Melbourne, Victoria, 3010, Australia

<sup>7</sup>Co-first author

\*Correspondence: tonkin@wehi.edu.au

<http://dx.doi.org/10.1016/j.chom.2015.11.004>

## SUMMARY

Transmissible stages of *Toxoplasma gondii* store energy in the form of the carbohydrate amylopectin. Here, we show that the  $\text{Ca}^{2+}$ -dependent protein kinase CDPK2 is a critical regulator of amylopectin metabolism. Increased synthesis and loss of degradation of amylopectin in CDPK2 deficient parasites results in the hyperaccumulation of this sugar polymer. A carbohydrate-binding module 20 (CBM20) targets CDPK2 to amylopectin stores, while the EF-hands regulate CDPK2 kinase activity in response to  $\text{Ca}^{2+}$  to modulate amylopectin levels. We identify enzymes involved in amylopectin turnover whose phosphorylation is dependent on CDPK2 activity. Strikingly, accumulation of massive amylopectin granules in CDPK2-deficient bradyzoite stages leads to gross morphological defects and complete ablation of cyst formation in a mouse model. Together these data show that  $\text{Ca}^{2+}$  signaling regulates carbohydrate metabolism in *Toxoplasma* and that the post-translational control of this pathway is required for normal cyst development.

## INTRODUCTION

*Toxoplasma gondii* is an obligate intracellular protozoan parasite of warm-blooded animals, including humans. Toxoplasmosis results from the ingestion of sporulated oocysts present in soil, water, or vegetables contaminated with cat feces, or by ingesting raw or undercooked meat harboring tissue cysts. Both stages can differentiate into rapidly dividing tachyzoite stages that are usually controlled by a protective immune response. However, in immunocompromised individuals severe systemic disease can occur, while in the developing fetus *Toxoplasma*

infection can cause spontaneous miscarriage, blindness, or congenital neurological defects, including epilepsy, mental retardation, and hydrocephaly (Hill et al., 2005; Torgerson and Mastriacovo, 2013).

Under immune pressure, a proportion of tachyzoites differentiate back into the relatively quiescent, slow-growing bradyzoites, which form latent cysts in muscle and CNS tissue that can persist for the lifetime of the infected host. Most chronic infections are asymptomatic, but bradyzoites can differentiate back to tachyzoites in CNS tissue of immunosuppressed individuals, leading to serious neurological disease and death if not treated. In addition, cyst formation in the retina is a significant cause of blindness (Glasner et al., 1992).

*Toxoplasma* tachyzoites can utilize both glucose and glutamine scavenged from the host cell to drive energy production (MacRae et al., 2012; Oppenheim et al., 2014; Blume et al., 2009), and following host cell egress, tachyzoites accumulate  $\gamma$ -aminobutyric acid, which may provide extracellular tachyzoites with a short-term energy reserve to fuel motility and invasion (MacRae et al., 2012). *Toxoplasma* tachyzoites also produce the storage polysaccharide amylopectin, which contains a backbone of  $\alpha(1\text{-}4)$ -linked glucose residues modified with  $\alpha(1\text{-}6)$ -linked branch points (Guérardel et al., 2005). Tachyzoites generally express very low levels of amylopectin unless stressed, but in contrast, bradyzoites and oocysts accumulate high levels of amylopectin granules in the cytoplasm (Coppin et al., 2003; Guérardel et al., 2005; Ferguson et al., 1974; Ferguson and Hutchison 1987). It has been postulated that amylopectin granules may be a long-term energy reserve during transmission to maintain parasite viability in low-nutrient niches and/or to drive rapid differentiation when they encounter favorable conditions. However, essentially nothing is known about how amylopectin accumulation and utilization is regulated in different *Toxoplasma* life cycle stages.

$\text{Ca}^{2+}$ -dependent protein kinases (CDPKs) are key mediators of  $\text{Ca}^{2+}$  signaling in apicomplexan parasites (Billker et al., 2009). They share a domain structure consisting of a variable N-terminal region, a kinase domain, and a calmodulin (CaM)-like domain containing  $\text{Ca}^{2+}$ -binding EF-hands. During  $\text{Ca}^{2+}$  signaling events,

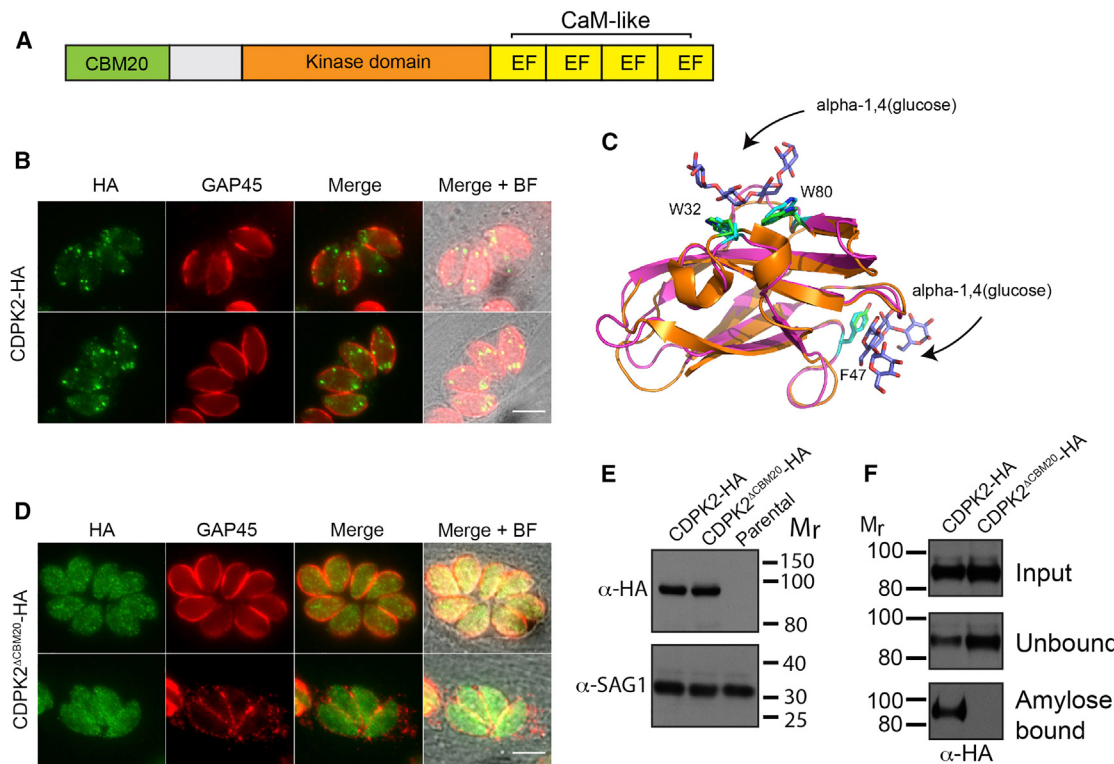


**Figure 1. CDPK2 Associates with Amylopectin via a CBM20 Domain**

(A) CDPK2 domain structure.

(B) Localization of CDPK2-HA in wild-type RH tachyzoites by IFA. Staining with anti-HA, peripheral marker anti-GAP45; BF, brightfield

(C) Homology model of CDPK2 (magenta) based on the CBM20 domain of Cyclodextrin Glycosyltransferase (PDB: 1eo5; orange). Carbohydrate ligand residues are shown: W32 and W80 in binding site 1; F47 in binding site 2.

(D) Localization of CDPK2<sup>ΔCBM20</sup>-HA Staining as for (B) above.

(E) Western blot for CDPK2-HA and CDPK2<sup>ΔCBM20</sup>-HA ectopically expressed in wild-type RH parasites. Staining with anti-HA and anti-SAG1 (loading control) antibodies.

(F) Western blot for CDPK2-HA and CDPK2<sup>ΔCBM20</sup>-HA applied to amylose-resin. Input, unbound, and amylose bound fractions are stained with anti-HA antibodies. All scale bars represent 5 μm. See also Figure S1.

Ca<sup>2+</sup> released from intracellular stores is bound by the EF-hands, leading to a conformational change in the CaM-like domain away from the kinase substrate binding pocket and kinase activation (Wernimont et al., 2010). Ca<sup>2+</sup> signaling and CDPK function in *Toxoplasma* and related apicomplexan parasites have previously been linked with parasite host cell egress (Garrison et al., 2012; Lourido et al., 2012; McCoy et al., 2012), invasion (Lourido et al., 2010), extracellular motility (Siden-Kiamos et al., 2006), and cell division (Morlon-Guyot et al., 2013). CDPKs also regulate *Plasmodium* stage differentiation in the mosquito life cycle (Billker et al., 2004; Sebastian et al., 2012).

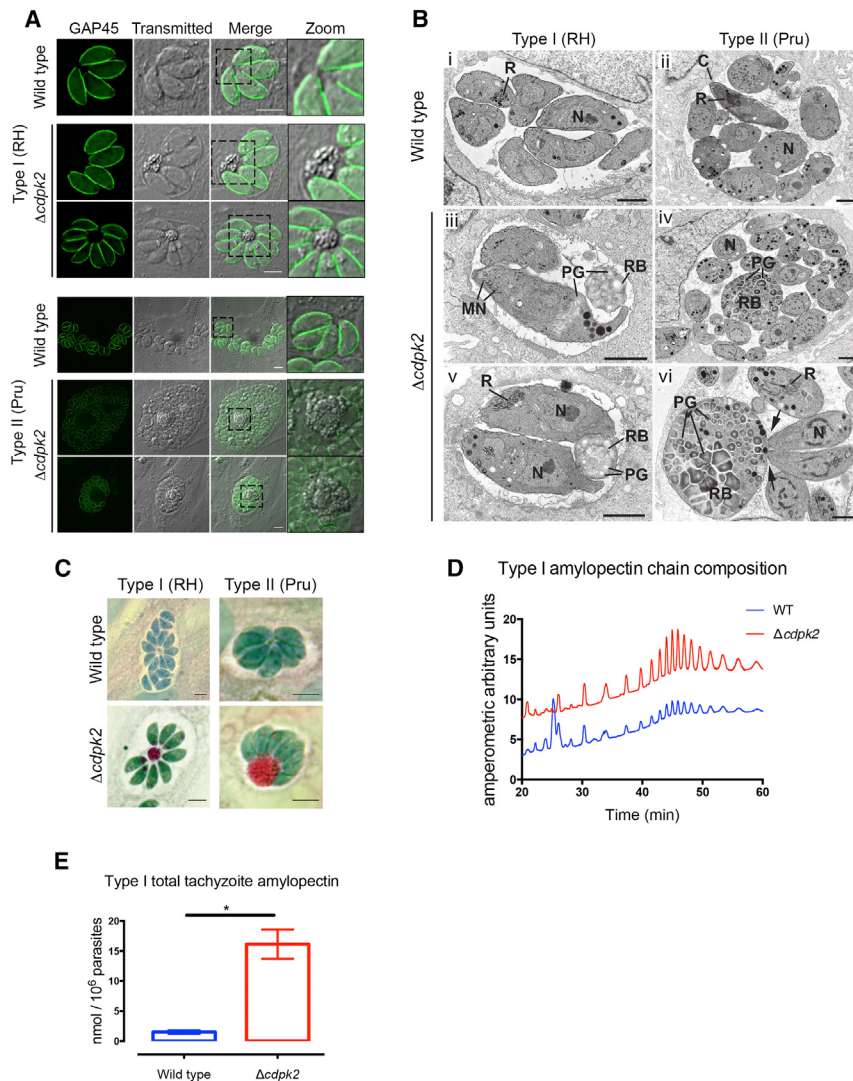
Here, we show that CDPK2 plays a key role in regulating amylopectin formation and degradation. Loss of CDPK2 leads to the hyper-accumulation of amylopectin in both tachyzoites and bradyzoites. This is particularly pronounced in bradyzoites, leading to massive ultrastructural changes and loss of viability and an inability to establish a chronic infection in mice. Our findings describe a signaling cascade that regulates *Toxoplasma* amylopectin storage, thus providing insights into the regulatory mechanisms essential for transmission of encysted parasites and their ability to establish infection.

## RESULTS

### The CBM20 Domain of CDPK2 Is Required for Correct Subcellular Targeting and Glucan Binding

During our investigations of Ca<sup>2+</sup> signaling in *Toxoplasma*, we noticed that CDPK2 contained a predicted N-terminal carbohydrate-binding module 20 (CBM20) that commonly binds to starch (Figures 1A and S1). The presence of this domain suggested a possible link between Ca<sup>2+</sup> signaling and carbohydrate metabolism via CDPK2. Indeed, a BLAST search of the EuthPathDB.org database, revealed that orthologs of CDPK2 are also found in the genomes of other coccidian species, which are known to produce amylopectin (Gajria et al., 2008).

To localize CDPK2, we tagged it with a triple HA epitope tag (CDPK2-HA) and expressed it ectopically in a Type I (RH strain) background. CDPK2-HA localized to a number of small puncta within the cytoplasm (Figure 1B). These puncta were also seen when the endogenous *cdpk2* gene was tagged (Figure S1B). To assess the potential function of the CBM20 domain, we generated a structural model of the CDPK2 CBM20 domain in complex with α-1,4-glucose (Figure 1C) based on previously



described bacterial CBM20 domains (Figure S1). This model identified W32, W80, and F47 as residues most likely to be important for the interaction with carbohydrate chains. A version of CDPK2 harboring W32L, W80L, and F47A mutations ( $CDPK2^{\Delta CBM20}$ -HA) no longer exhibited the distinct punctate pattern but rather was distributed throughout the cytoplasm, although some puncta were still evident (Figure 1D). This change in localization was not a result of differences in expression level between wild-type and mutant proteins (Figure 1E). Indeed, a pixel intensity heatmap showed that while CDPK2-HA is highly concentrated in its discrete puncta, the expression of  $CDPK2^{\Delta CBM20}$ -HA is overall quantitatively less dense throughout the body of the tachyzoites (Figure S1C).

To test if the CBM20 domain of CDPK2 facilitates amylopectin binding, cell lysates from tachyzoites expressing either CDPK2-HA or  $CDPK2^{\Delta CBM20}$ -HA were applied to amylose (un-branched  $\alpha$ -(1,4) glucan) affinity matrix. While CDPK2-HA bound to the amylose resin, the  $CDPK2^{\Delta CBM20}$ -HA protein showed no detectable binding (Figure 1F). These data suggest that CDPK2 is recruited to the amylopectin granules, via its

**Figure 2. Knockout of CDPK2 Leads to Aberrant Amylopectin Accumulation in *Toxoplasma* Tachyzoites**

(A) Accumulation of granular deposits in RH: $\Delta cdpk2$  and Pru: $\Delta cdpk2$  tachyzoites, visualized by IFA (staining with peripheral marker anti-GAP45) and bright-field microscopy.

(B) Transmission electron micrographs of wild-type RH (Bi), Pru (Bii) RH: $\Delta cdpk2$  ([Biii] and [Bvi]), and Pru: $\Delta cdpk2$  ([Biv] and [Bv]) tachyzoites. C, conoid; MN, micronemes; N, nucleus; PG, polysaccharide granule; RB, residual body; R, rhoptry. Scale bars represent 2  $\mu$ m.

(C) PAS staining of RH: $\Delta cdpk2$  and Pru: $\Delta cdpk2$ .

(D) Analysis of amylopectin composition in wild-type RH and RH: $\Delta cdpk2$  tachyzoites by HPAEC.

(E) Quantification of amylopectin levels in RH and RH: $\Delta cdpk2$ . Data represent the mean with SEM from six biological replicates from two independent experiments (\*p < 0.05, t test). All scale bars represent 5  $\mu$ m unless otherwise indicated. See also Figures S2 and S3. Error bars are  $\pm$  SEM.

functional CBM20 domain, accounting for the punctate localization pattern.

### CDPK2 Deficiency Leads to Abnormal Amylopectin Storage in *Toxoplasma* Tachyzoites

To investigate the function of CDPK2 and how it relates to amylopectin metabolism, we created  $cdpk2$ -deficient Type I (RH) and Type II (Pru) lines (Figure S2A) in  $\Delta ku80$  strains (Fox et al., 2011; Huynh and Carruthers, 2009). Both RH: $\Delta cdpk2$  and Pru: $\Delta cdpk2$  lines infected HFFs to the same extent as wild-type parasites, but intracellular  $\Delta cdpk2$  tachyzoites were observed to accumulate granules at their basal end and additional, larger

granules within the parasite residual body (Figure 2A), which was further enhanced in the type II background. Analysis of the  $\Delta cdpk2$  lines by transmission electron microscopy showed that granular deposits corresponded to semi-crystalline polysaccharide granules (PGs), which were completely absent from the wild-type strains (Figure 2B). Consistent with our observations by light microscopy, these deposits were found both at the basal end of the parasites as well as in engorged residual bodies, which in some cases were still attached to dividing parasites (Figures 2Bii–2Bvi). To confirm the polysaccharide nature of these granules, we performed Periodic acid-Schiff (PAS) staining, which marks carbohydrates deposits in cells. We observed that while wild-type parasites showed no staining or only very small puncta, both RH: $\Delta cdpk2$  and Pru: $\Delta cdpk2$  parasites showed very pronounced staining of multiple puncta, consistent with the granules seen in the EM studies (Figure 2C).

To confirm that  $\Delta cdpk2$  parasites accumulate amylopectin, granules were extracted from parental RH and RH: $\Delta cdpk2$  tachyzoites. Glucan chains were released by isoamylase digestion and analyzed by high-pH anion-exchange chromatography

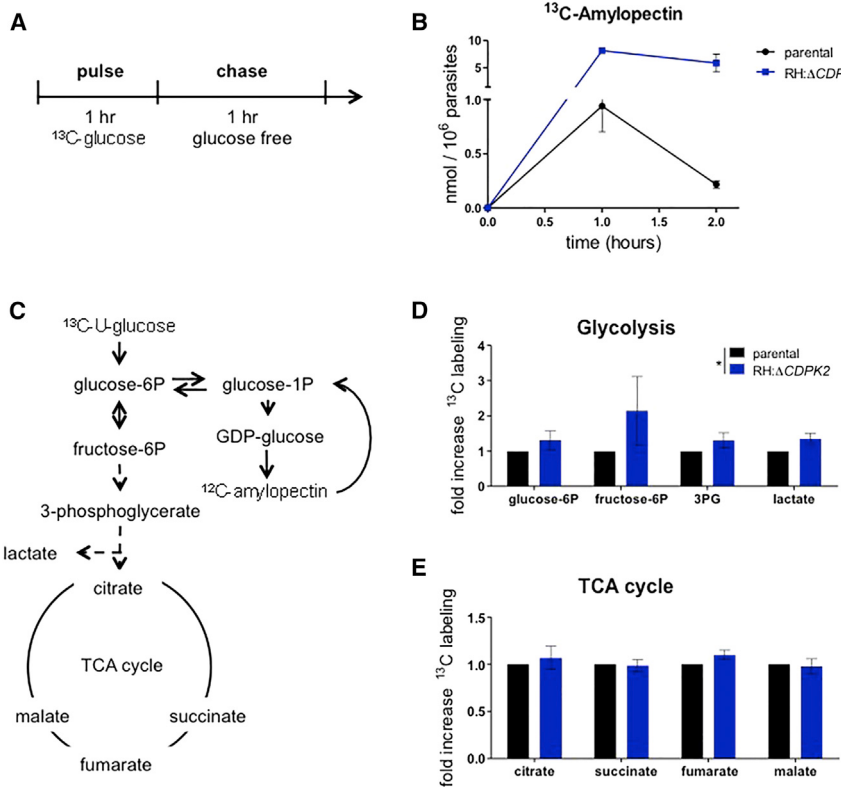


**Figure 3. RH:Δcdpk2 Parasites Accumulate Amylopectin through Increased Synthesis and Attenuated Degradation**

(A) Pulse-chase labeling of amylopectin. Extracellular parasites were labeled for 1 hr with <sup>13</sup>C-U-glucose and then glucose starved for 1 hr.

(B) Turnover of <sup>13</sup>C-amylopectin in RH and RH:Δcdpk2 (\*p < 0.05, t test at 1 hr and 2 hr). Data represent mean with SEM of three independent labeling reactions.

(C) Schematic of <sup>13</sup>C-U-glucose labeling of intracellular metabolites.

(D) Fold incorporation of <sup>13</sup>C into glycolytic metabolites in RH and RH:Δcdpk2 (\*p = 0.07, two-way ANOVA).

(E) Fold incorporation of <sup>13</sup>C into TCA cycle intermediates in RH and RH:Δcdpk2 strains. Data shown are means with SEM from three independent experiments. Error bars are ± SEM.

(HPAEC) (Figure 2D). This showed that parental and Δcdpk2 tachyzoites contained poly-dispersed glucan chains having a degree of polymerization (DP) of 4–20, consistent with previous analyses (Guérardel et al., 2005). Methylation linkage analysis of the total polysaccharide fraction of RH:Δcdpk2 parasites confirmed the presence of predominantly α-1,4 linked glucose with intermittent α-1,6 linked branch points, again indicative of amylopectin (Figure S3A) (Pettolino et al., 2012). To quantify differences in amylopectin abundance between wild-type and Δcdpk2 parasites, we digested boiled cell lysates of purified type I tachyzoites with α-glucosidase and measured the released glucose by gas chromatography-mass spectrometry (GC/MS). Amylopectin abundance was elevated approximately 10-fold in Δcdpk2 tachyzoites (Figure 2E). We, however, only saw mild defects in growth of Δcdpk2 tachyzoites by plaque (Figure S3B) and competition assay (Figure S3C).

#### CDPK2 Regulates Synthesis and Degradation of Amylopectin and Causes an Increase in Glycolytic Flux

To understand the effect of loss of CDPK2 on synthesis and degradation of amylopectin, freshly egressed RH parental and RH:Δcdpk2 parasites were labeled with <sup>13</sup>C-glucose for 1 hr and then resuspended in glucose-free medium for a further hour (Figure 3A). The incorporation and subsequent chase of <sup>13</sup>C into amylopectin was determined by GC/MS analysis of α-glucosidase-digested hot water extracts (Figure 3B). The RH:Δcdpk2 line synthesized approximately eight times as much <sup>13</sup>C-amylopectin as the parental strain during the pulse period (Figure 3B). Conversely, the RH:Δcdpk2 parasites did not degrade their amylopectin pool during the subsequent glucose

starvation period, in contrast to wild-type parasites, which completely turned over their <sup>13</sup>C-labeled pool of amylopectin (Figure 3B). These data suggest that loss of CDPK2 results in increased channeling of exogenous glucose into amylopectin synthesis, as well as reduced amylopectin degradation.

To determine whether CDPK2 regulates other pathways in central carbon metabolism, extracellular parental and RH:Δcdpk2 tachyzoites were labeled with <sup>13</sup>C-glucose for 1 hr, and the incorporation of <sup>13</sup>C into a range of intermediates in glycolysis and the TCA cycle was analyzed by GC/MS (Figure 3C). Increased labeling of all glycolytic intermediates was observed in RH:Δcdpk2 parasites compared to the parental strain (Figure 3D), while labeling of TCA cycle intermediates remained unchanged (Figure 3E). These data are consistent with reduced turnover of pre-existing pools of unlabeled amylopectin in RH:Δcdpk2 tachyzoites, which leads to increased efficiency of labeling of hexose phosphates in the Δcdpk2 mutant.

#### CDPK2 Kinase Activity and a Functional CBM20 Are Required for Regulation of Amylopectin Homeostasis

To determine if the CBM20 domain of CDPK2 is critical to the function of CDPK2 in regulating amylopectin levels, RH:Δcdpk2 parasites were complemented with either wild-type CDPK2-HA or CDPK2<sup>ΔCBM20</sup>-HA. Wild-type CDPK2-HA showed the expected punctate staining pattern seen previously, and its expression successfully complemented the Δcdpk2 phenotype, with parasites not producing amylopectin granules visible by light microscopy (Figure 4A). The mis-targeted CDPK2<sup>ΔCBM20</sup>-HA mutant, however, did not complement the Δcdpk2 phenotype, with CDPK2<sup>ΔCBM20</sup>-HA:Δcdpk2 parasites still accumulating large amylopectin granules (Figure 4B). These data strongly suggest that targeting of CDPK2 to amylopectin is required for the regulation of amylopectin synthesis and turnover.

Kinases regulate biological processes either by phosphorylating target effector proteins or by acting as a scaffold or allosteric regulator of protein complexes (Behnke et al., 2012;

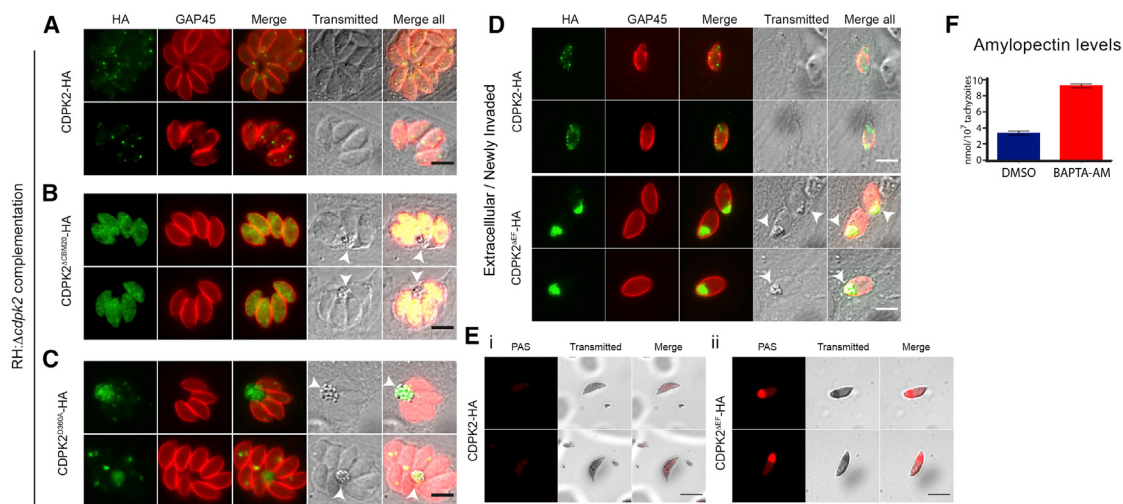


**Figure 4. Kinase Activity, Interaction with Amylopectin, and Functional EF Hands Are Required for Degradation of Amylopectin by CDPK2**

(A) IFA of RH:Δcdpk2 tachyzoites complemented with CDPK2-HA. Staining with anti-HA and peripheral marker anti-GAP45.

(B) IFA of RH:Δcdpk2 tachyzoites complemented with CDPK2<sup>ΔCBM20</sup>-HA.

(C) IFA of RH:Δcdpk2 tachyzoites complemented with CDPK2<sup>D360A</sup>-HA.

(D) IFA of extracellular/newly invaded RH:Δcdpk2 tachyzoites complemented with CDPK2<sup>ΔEF</sup>-HA.

(E) PAS stain fluorescence in extracellular RH:Δcdpk2 parasites complemented with CDPK2-HA (Ei), and CDPK2<sup>ΔEF</sup>-HA (Eii).

(F) Accumulation of amylopectin in extracellular wild-type RH parasites, treated with Ca<sup>2+</sup> chelator BAPTA-AM or vehicle only (DMSO), quantified by GC/MS analysis. Data represent the mean with SEM of three independent reactions (\*p < 0.005, t test). White arrowheads indicate sites of granular accumulation. All scale bars represent 5 μm. See also Figure S4. Error bars are ± SEM.

(Fleckenstein et al., 2012). To assess whether the enzymatic activity of CDPK2 is required for the function of this kinase, we complemented RH:Δcdpk2 parasites with a catalytically inactive mutant of CDPK2 (CDPK2<sup>D360A</sup>-HA). This mutant did not complement the Δcdpk2 phenotype despite the fact that the CDPK2<sup>D360A</sup>-HA protein appeared to be strongly associated with the large amylopectin granules (Figure 4C). Therefore, the kinase activity of CDPK2 is required for the regulation of amylopectin turnover and further suggests that CDPK2 associates with amylopectin in situ.

#### Amylopectin Levels in *Toxoplasma* Are Regulated by Ca<sup>2+</sup> Signaling

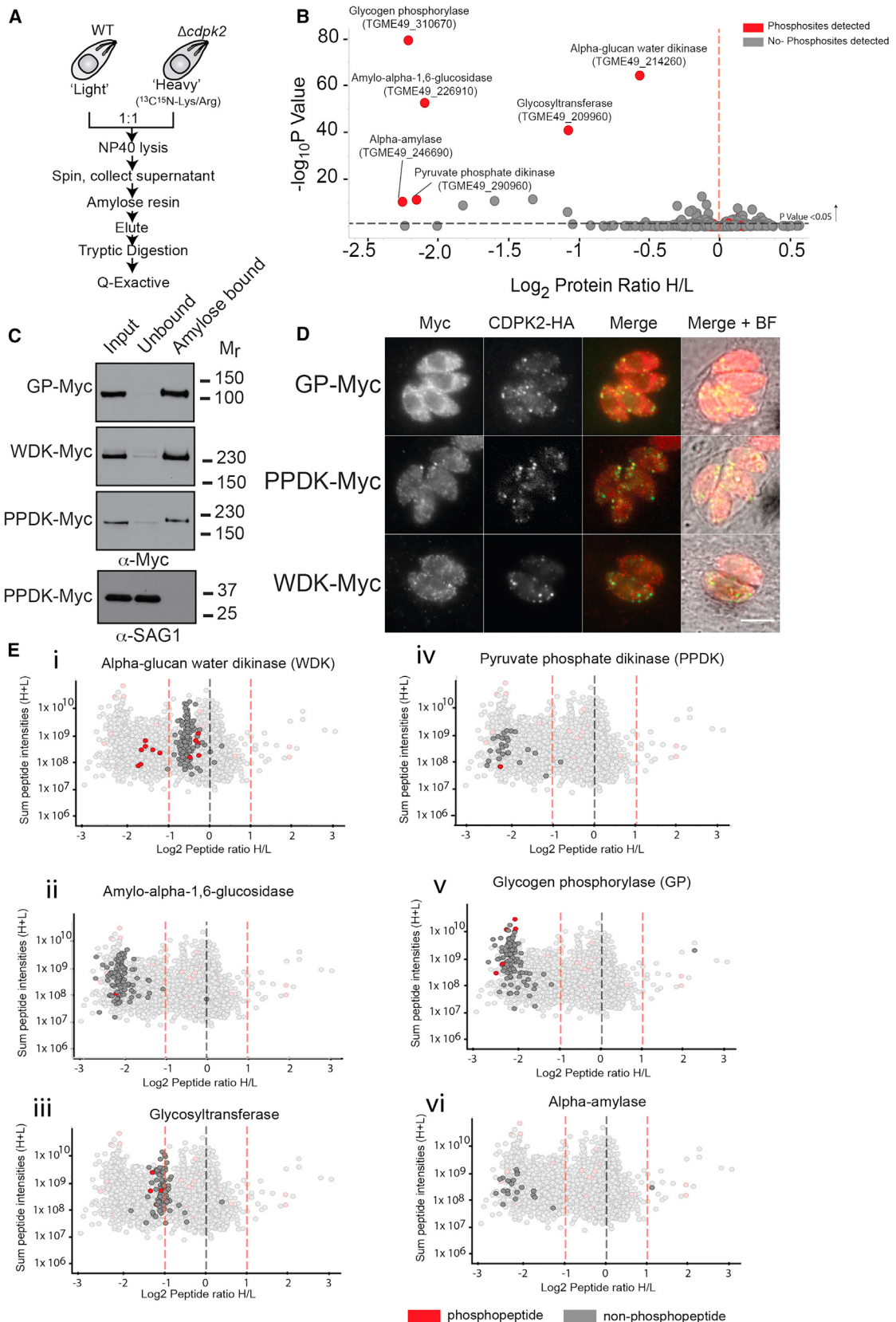
Given that the catalytic activity of CDPKs is directly regulated by Ca<sup>2+</sup>, we investigated whether Ca<sup>2+</sup> levels regulate amylopectin levels through CDPK2 activity (Wernimont et al., 2010). To address this, we aligned the EF hands of CDPK2 with EF hands of other CDPKs known to regulate Ca<sup>2+</sup>-dependent processes (CDPK1 and 3) and *Toxoplasma* CaM (Figure S4A) (Lourido et al., 2012; Wernimont et al., 2010). This alignment identified conserved residues in the CDPK2 EF hands predicted to be essential for Ca<sup>2+</sup> binding. A CDPK2<sup>ΔEF</sup>-HA protein with mutations in these sites was unable to complement the RH:Δcdpk2 phenotype when tachyzoites were either extracellular or newly invaded (Figure 4D). This was also evident by PAS fluorescent staining showing the accumulation of amylopectin in extracellular RH:Δcdpk2:CDPK2<sup>ΔEF</sup>-HA tachyzoites, but not in RH:Δcdpk2:CDPK2-HA tachyzoites (Figures 4Ei and 4Eii). Furthermore, CDPK2<sup>ΔEF</sup>-HA showed localization to sites of amylopectin accumulation in RH:Δcdpk2 parasites (Figure 4D). Interestingly, we noticed that intracellular, replicating

RH:Δcdpk2:CDPK2<sup>ΔEF</sup>-HA parasites that had undergone one to two rounds of division had lost these large amylopectin stores (Figures S4B and S4C).

We also measured the effect of quenching of Ca<sup>2+</sup> signaling by BAPTA-AM on the mobilization of amylopectin stores in glucose-starved extracellular tachyzoites (Carruthers and Sibley, 1999; Nebl et al., 2011). BAPTA-AM treatment conferred retention of amylopectin when compared with vehicle-only (DMSO) controls; resulting in approximately 9 nmol amylopectin per 10<sup>7</sup> tachyzoites as compared to 3.5 nmol in DMSO-treated parasites (Figure 4F). Together, these data strongly suggest that intracellular Ca<sup>2+</sup> levels and the turnover of amylopectin are linked via CDPK2 in extracellular *Toxoplasma* tachyzoites.

#### Quantitative Proteomics Identifies Proteins Involved in Amylopectin Metabolism and Phosphorylation Events Potentially Regulated by CDPK2

Given that the catalytic activity of CDPK2 and its association with amylopectin are both critically required for regulation of amylopectin turnover, we reasoned that the substrates of CDPK2 must also possess the ability to associate with amylopectin. We therefore set out to identify all proteins that can associate with amylopectin and the phosphorylation sites on these proteins that were influenced by CDPK2. We developed a quantitative proteomic approach where we grew RH:Δcdpk2 tachyzoites with “heavy” Lys and Arg, while keeping wild-type RH in “light” (regular) Lys and Arg. We mixed NP-40 lysed samples at a 1:1 ratio, applied them to amylose resin, and analyzed bound fractions by mass spectrometry (Figure 5A). Proteomic analysis identified 603 unique proteins (Table S2). Significantly, eleven of these proteins that differed in amount between the wild-type RH and



(legend on next page)

RH: $\Delta cdpk2$  lysates are predicted to be involved in starch breakdown or synthesis, and we detected phosphorylation sites on six of these proteins (Figure 5B). Given that SILAC ratios of these proteins deviated from the 1:1 ratio of initial mixing, with a bias of peptides coming from the wild-type (“light” labeled) parasites, we wondered if our method of solubilization had serendipitously allowed us to identify proteins that bound to starch with more confidence. Because  $\Delta cdpk2$  tachyzoites produce huge amounts of amylopectin, we wondered whether the greater amount of this sugar polymer in  $\Delta cdpk2$  parasites rendered more of the starch-binding proteins insoluble under NP-40 lysis conditions. To test this and to make sure that CDPK2 was not affecting the expression level of these proteins, we tagged glycogen phosphorylase (GP), pyruvate phosphate dikinase (PPDK), and alpha-glucan water dikinase (WDK) with a triple-myc epitope tag in both wild-type and  $\Delta cdpk2$  tachyzoites. Loss of CDPK2 did not change the overall amount of these proteins (Figure S5A) but increased the NP-40 insolubility of GP under the NP-40 lysis conditions (Figure S5B). Furthermore, by IFA, GP associates strongly with amylopectin granules in the  $\Delta cdpk2$  background (Figure S5C), supporting the premise that GP associates strongly with amylopectin stores in *Toxoplasma* tachyzoites, thus explaining why starch-binding proteins are found in less abundance in  $\Delta cdpk2$  in our proteomic experiments. We also showed that GP, PPDK, and WDK all bind strongly to amylose resin in vitro assays (Figure 5C), and moreover, all partially co-localize with CDPK2 by IFA (Figure 5D), therefore validating our identification of *Toxoplasma* starch-binding proteins.

To further examine the role that CDPK2 may be playing in regulating the activity of proteins involved in amylopectin synthesis and degradation, we analyzed the ratios ( $\Delta cdpk2$ :wild-type) of individual phosphopeptides and non-phosphorylated peptides in proteins where phosphorylation was detected (Figure 5E). Interestingly, several phosphopeptides from WDK (a protein predicted to be involved in starch breakdown) appeared to be less abundant in  $\Delta cdpk2$  (heavy) lysates as compared to wild-type, four of which appeared to be statistically significant (Figure 5Ei and S6A). We could also detect phosphopeptides from amylo- $\alpha$ -1,6-glucosidase (Figure 5Eii), glycosyltransferase (Figure 5Eiii), PPDK (Figure 5Eiv), GP (Figure 5Ev), and  $\alpha$ -amylase (Figure 5Evi), although sites on the latter protein were not quantifiable as they were only detected in one replicate and thus are not shown (Table S2). In several cases, some phosphopeptides appeared to be less abundant, compared to non-phosphopeptides in  $\Delta cdpk2$  tachyzoites, but these were not considered significant upon calculating confidence intervals (Figure S6A). We also analyzed the occupancy of phosphorylation on particular sites

of WDK by identifying phosphorylated and non-phosphorylated versions of the same peptide and comparing their ratios. While we could clearly see a difference in relative abundance between phosphorylated and non-phosphorylated versions of four peptides from WDK, it should be noted that this is not quantifiable using experimental techniques at hand due to the change in chemical properties upon phosphorylation (Figure S6B).

We also functionally validated our proteomic identification of amylopectin binding proteins by deleting the *GP* gene in RH using CRISPR/Cas9. *Agp* tachyzoites showed accumulation of amylopectin similar to the phenotype observed in the RH: $\Delta cdpk2$  strain (Figure S5D).

### CDPK2 Can Directly Phosphorylate PPDK as Observed by Chemical Genetics

To see if the phosphorylated proteins identified above are direct substrates of CDPK2, we utilized a recently described kinase substrate capture technique (Allen et al., 2007; Bishop et al., 2000; Blethow et al., 2008; Lourido et al., 2013). Substrate capture relies on genetically sensitizing the target kinase by mutating the “gatekeeper” residue of the ATP binding pocket to alter its shape and make it accessible to bulky ATP analogs (Figure 6Ai), thereby allowing the kinase to specifically “thiophosphorylate” its substrates (Figure 6Aii). We tested whether PPDK could be thiophosphorylated by CDPK2. PPDK was chosen prior to us having performed the quantitative proteomics, on the basis that it contains a CBM20 domain like CDPK2, while also binding strongly to amylose resin (Figure 5C) and partially co-localizes with CDPK2 (Figure 5D).

RH: $\Delta cdpk2$  parasites were complemented with full-length cDNA copies of wild-type or analog-sensitive (CDPK2<sup>M314G-HA</sup>) alleles expressed from the tubulin promoter and integrated at the *uprt* locus (Figure 6B). We desensitized native CDPK1, which is naturally analog-sensitive by allelic swap (CDPK1<sup>G128M-Ty</sup>) (Figure 6B). Ectopic CDPK2<sup>WT-HA</sup> and CDPK2<sup>M314G-HA</sup> (hereafter referred to as CDPK2<sup>M</sup> and CDPK2<sup>G</sup>, respectively) are functional as they are able to complement the RH: $\Delta cdpk2$  phenotype (Figures 6Ci and 6Cii). The analog insensitivity of the desensitized CDPK1<sup>G128M-Ty</sup> mutant was confirmed by showing no retardation of A23187-stimulated egress following 3MB-PP1 inhibition (data not shown) (Lourido et al., 2010). Western blotting confirmed their expression (Figure 6D).

To monitor the ability of CDPK2 to thiophosphorylate PPDK, we endogenously Myc-tagged PPDK in both the CDPK2<sup>G</sup> and CDPK2<sup>M</sup> backgrounds (CDPK2<sup>G</sup>:PPDK-Myc and CDPK2<sup>M</sup>:PPDK-Myc, respectively) and confirmed tagging by western blot (Figure 6D) and IFA (not shown). We performed thiophosphorylation reactions on cell lysates, followed by

**Figure 5. Quantitative Proteomics Reveals Potential Substrates of CDPK2**

- (A) Strategy used for quantitative proteomics of  $\Delta cdpk2$  and wild-type parasites.
- (B) Volcano plot of all amylose-bound proteins identified and their SILAC ratios. Red circles indicate that phosphopeptides were detected for these proteins. Grey indicates that only non-phosphorylated peptides were detected. Proteins with a  $-\log_{10} p$  value of 1.3 or greater ( $p$  value of  $\leq 0.05$ ) were deemed differentially abundant.
- (C) Western blot for amylose binding of GP-Myc, PPDK-Myc, and WDK-Myc. Input, unbound, and amylose-bound fractions were stained with anti-Myc antibodies. SAG1 was used as a negative control for amylose binding.
- (D) Partial co-localization of CDPK2-HA with WDK-Myc, PPDK-Myc, and WDK-Myc, detected by IFA with anti-HA and anti-Myc antibodies. BF, brightfield.
- (E) Proteins ([Ei]–[Evi]) predicted to be involved in starch degradation contain phosphopeptides (shown in red). Phosphopeptides for  $\alpha$ -amylase (Evi) are not shown, as they were only identified in one replicate, and thus a  $p$  value could not be calculated. All scale bars represent 5  $\mu$ m. See also Figures S5 and S6.

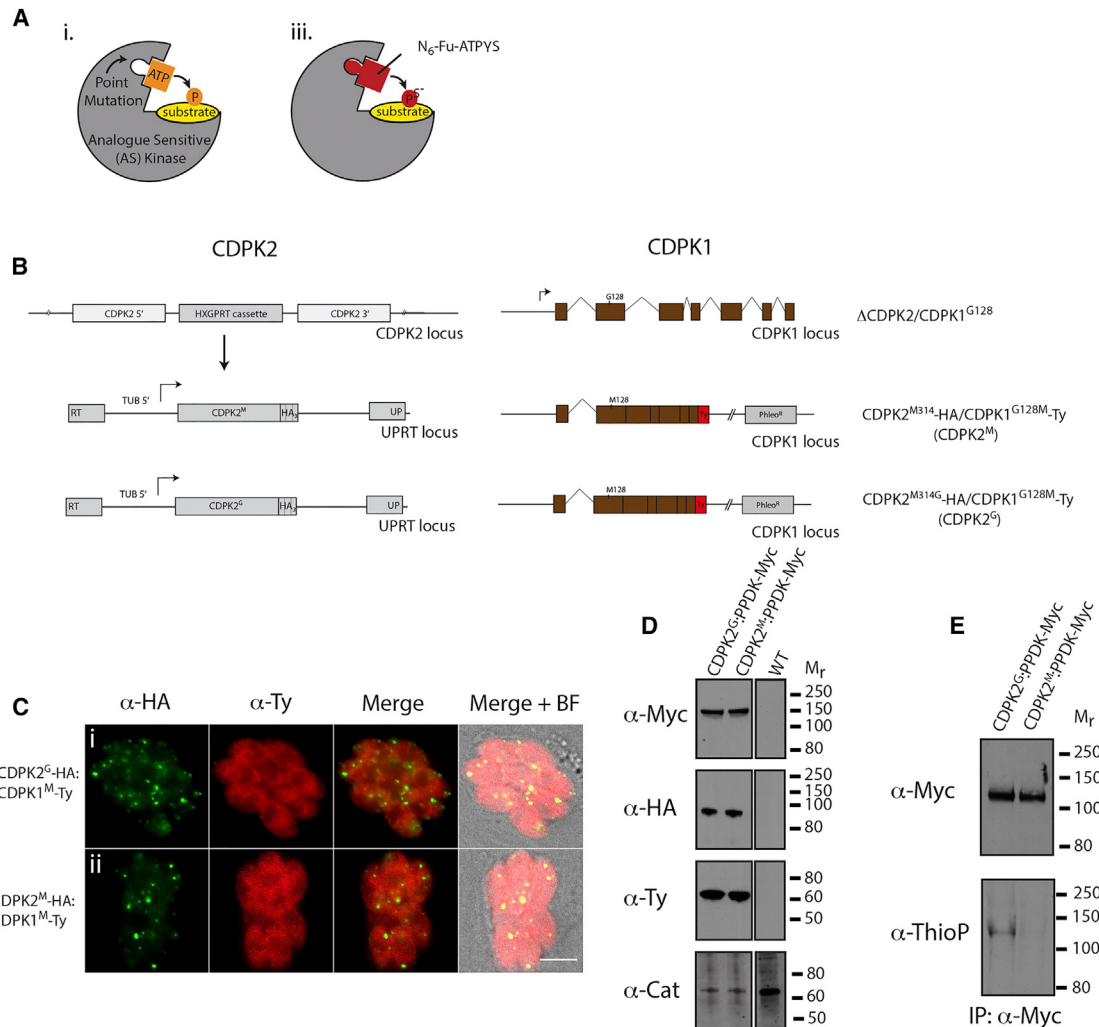


**Figure 6. CDPK2 Can Thiophosphorylate PPDK**

(A) Schematic showing the principle of analog-sensitive kinases. A specific point mutation in the ATP-binding pocket of a kinase can make it “analogue sensitive”—able to make use of ATP analogs to thiophosphorylate its substrates.

(B) Strategy used to generate analog-sensitive CDPK2-expressing parasites.

(C) Localization of CDPK1<sup>M</sup>-Ty, CDPK2<sup>M</sup>-HA, and CDPK2<sup>G</sup>-HA by IFA (detected with anti-HA and anti-Ty antibodies). Scale bars represent 5  $\mu$ m.

(D) Western blot of tagged proteins in CDPK2<sup>G</sup>-HA:PPDK-Myc and CDPK2<sup>M</sup>-HA:PPDK-Myc parasites (detected with anti-Myc, -HA, -Ty and -Catalase [loading control] antibodies).

(E) Thiophosphorylation of PPDK-Myc in CDPK2<sup>G</sup> but not CDPK2<sup>M</sup>-expressing parasites. PPDK-Myc and its thiophosphorylation were detected with anti-Myc and anti-thiophosphate ester (anti-ThioP) antibodies, respectively. The blot is representative of four independent experiments.

immunoprecipitation of PPDK-Myc, and observed that PPDK-Myc was thiophosphorylated in the presence of CDPK2<sup>G</sup>, but not CDPK2<sup>M</sup> (Figure 6E), suggesting that CDPK2 can directly phosphorylate PPDK.

#### CDPK2 Loss Leads to Massive Amylopectin Accumulation and Death in Bradyzoites

Amylopectin is natively found in chronic-stage bradyzoites; we therefore wondered if CDPK2 plays an important role in regulating the development of amylopectin stores at this stage. We therefore differentiated Pru and Pru: $\Delta$ cdpk2 tachyzoites into bradyzoites by high-pH shock over 14 days. Over this time period, wild-type parasites exhibited a mild increase in PAS staining,

which was detected as small, granular staining throughout the body of the developing bradyzoite (Figure 7A). In contrast, developing Pru: $\Delta$ cdpk2 bradyzoites accumulated massive amylopectin granules within 2 days (Figure 7A). These deposits continued to accumulate through to day 7. To assess the effects of this gross accumulation on parasite morphology, we performed IFAs on parasites 14 days post-bradyzoite induction (Figure 7B). We confirmed successful bradyzoite induction by observing GFP expression from the bradyzoite-specific LDH2 promoter (Fox et al., 2011), alongside expression of the bradyzoite surface marker SRS9, and observed nuclear morphology by DAPI staining. As expected, Pru parasites had successfully differentiated from tachyzoites into bradyzoites,

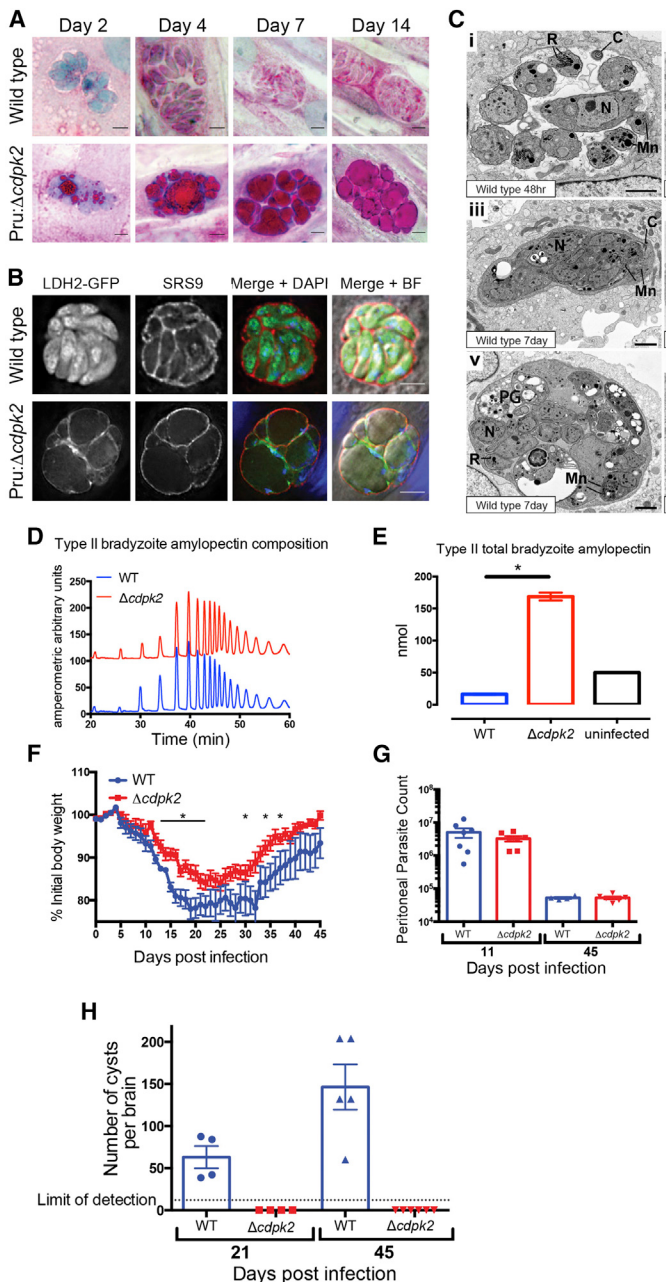


**Figure 7. CDPK2 Is Important for the Development of *Toxoplasma* Bradyzoites In Vitro and In Vivo**

(A) PAS staining of Pru and Pru:Δcdpk2 parasites stimulated to differentiate into bradyzoites by pH shock over 14 days.

(B) IFA of Pru and Pru:Δcdpk2 parasites subjected to pH shock for 14 days. Differentiation tracked by GFP expression driven by the LDH2 promoter (green) and the bradyzoite surface marker SRS9 (red). Staining with anti-SRS9 and DAPI (blue).

(C) Transmission electron micrographs of Pru ([Ci], [Cii], and [Cv]) and Pru:Δcdpk2 ([Cii], [Civ], and [Cvi]) parasites subjected to pH shock for indicated time periods. C, conoid; MN, micronemes; N, nucleus; PG, polysaccharide granule; R, rhoptry. Scale bars represent 1 μm.

(D) Analysis of amylopectin composition in wild-type Pru and Pru:Δcdpk2 bradyzoites by HPAEC.

(E) Quantification of amylopectin levels in Pru and Pru:Δcdpk2. Data represent the mean with SEM from three biological replicates from two independent experiments (\*p < 0.05, t test).

(F) Weight loss in Pru- and Pru:Δcdpk2-infected C57BL/6 mice (\*p < 0.05 on days 13–22, 30, 34, and 37, t tests).

(G) Acute stage tachyzoite burden in Pru- and Pru:Δcdpk2-infected C57BL/6 mice.

(H) Number of cysts in brain homogenates of Pru- and Pru:Δcdpk2-infected C57BL/6 mice. Mice were sacrificed at 21 and 45 days post-infection, (n = 4, day 21; n = 6, day 45). Error bars are ± SD. All scale bars: 5 μm unless otherwise indicated. See also Figure S7.

showing expression of GFP and SRS9, and a more basal nuclear position (Figure 7B). Strikingly, while Pru:Δcdpk2 parasites showed successful bradyzoite differentiation, developing bradyzoites were rounded and massively enlarged (Figure 7B). Indeed, the cytosol of Pru:Δcdpk2 bradyzoites, as detected by GFP, and nuclear staining, appeared to be largely displaced by the amylopectin granules, with remnants of the cytoplasm and nucleus being pressed to the periphery of parasites (Figure 7B). To investigate this further, Pru:Δcdpk2 bradyzoites were analyzed by transmission electron microscopy (Figure 7C). Ultrastructural examination of Pru wild-type parasites differentiated for 48 hr revealed typical tachyzoite/early bradyzoite morphology at this early time point (Figure 7Ci). In contrast, Pru:Δcdpk2 para-

sites showed huge deposits of PGs already massively distorting the parasite shape at this early time point (Figure 7Cii). At day 7, wild-type parasites exhibited more features typical of bradyzoites, such as an increase in micronemal number (Mn) and electron-dense rhoptries (R) and the appearance of some amylopectin granules (PG) (Figures 7Ciii and 7Cv). Pru:Δcdpk2 parasites, however, showed few features suggestive of viable bradyzoites, with cell bodies containing overwhelming deposits of PGs (Figures 7Civ and 7Cvi). Where organelles were

visible, they appeared pushed to the parasite periphery and distorted in shape.

To analyze the bradyzoite amylopectin composition, amylopectin granules were extracted from wild-type Pru and Pru:Δcdpk2 bradyzoites that had been differentiated for 5 days. Glucan chains were released by amylase digestion, and analyzed by HPAEC and carbohydrate linkage analysis (Figure 7D). Both wild-type and Δcdpk2 bradyzoites contained glucan chains with a DP of 4–20, indicative of amylopectin. Total α-amylase digestion of the amylopectin fraction of wild-type and Δcdpk2 bradyzoites, indicated a 10-fold increase in amylopectin abundance in Δcdpk2 bradyzoites (Figure 7E).

### CDPK2 Is Required for Formation of Bradyzoites In Vivo

To investigate the consequences of loss of CDPK2 and dysregulation of amylopectin metabolism on virulence and generation of a chronic infection, C57BL/6 mice were infected intra-peritoneally with either Pru wild-type or Pru: $\Delta$ cdpk2 tachyzoites and body weight, and symptoms were measured over a 45-day period (Figure 7F). Pru: $\Delta$ cdpk2-infected mice lost significantly less weight ( $p < 0.05$  on days 13–22, 30, 34, and 37;  $t$  test) than mice infected with the wild-type parasites (Figure 7F). However, the total tachyzoite burden in the peritoneal cavity was similar for both wild-type and Pru: $\Delta$ cdpk2 infections (Figure 7G), suggesting that CDPK2 is not a major determinant of tachyzoite virulence. Accordingly, blood parameters, spleen weight, and numbers of peritoneal infiltrate immune cells showed no difference between wild-type and  $\Delta$ cdpk2-infected animals (Figure S7). In contrast, we were unable to detect a single cyst within Pru: $\Delta$ cdpk2-infected animals either by looking for GFP (under the bradyzoite-specific LDH2-promoter) or by direct microscopic examination, while wild-type parasites showed an expected increase in cyst number over 45 days of infection (Figure 7H). These observations suggest that loss of CDPK2 leads to the catastrophic accumulation of amylopectin in bradyzoites, leading to parasite death and abrogation of cyst formation. The regulation of amylopectin formation through CDPK2 is thus essential for the development and persistence of cysts during chronic infection.

### DISCUSSION

The accumulation of amylopectin is a defining feature of encysting stages of *Toxoplasma* and other apicomplexan species, but until now, very little was known about the signaling pathways regulating its synthesis or degradation or its broader role in the control of flux through carbon metabolism pathways. Here we provide an example of  $\text{Ca}^{2+}$ -dependent regulation of carbohydrate metabolism in apicomplexan parasites via CDPK2. This work therefore describes a mechanism by which pathogens regulate energy metabolism during establishment of chronic infection.

Our metabolomic data shows that loss of CDPK2 leads to increased synthesis and decreased degradation of amylopectin. This suggests that CDPK2 activity downregulates the shunting of glucose into amylopectin and upregulates the mobilization of amylopectin, and thereby the generation of hexose-phosphates.  $^{13}\text{C}$ -glucose labeling studies further suggest that amylopectin turnover is coupled to glucose uptake and major pathways of energy generation. In particular, disruption of amylopectin synthesis and degradation appears to directly impact on glycolytic fluxes, suggesting that amylopectin may play a role as both a long-term polysaccharide reserve under conditions of nutrient limitation, and a dynamic short-term reserve of hexose precursors. Our data also suggest that dividing tachyzoites have small pool of amylopectin, which is rapidly turned over, a process that requires CDPK2.

Our data also suggest that  $\text{Ca}^{2+}$  signaling, via CDPK2 activity, regulates these amylopectin levels in *Toxoplasma*. From this and recent work by other groups, it is now clear that *Toxoplasma*  $\text{Ca}^{2+}$  signaling, through the action of CDPKs, is not limited to regulating parasite motility but also regulates other processes

that are important for establishing and maintaining infection (Morlon-Guyot et al., 2013). But why does *Toxoplasma* want to link amylopectin synthesis and degradation to intracellular  $\text{Ca}^{2+}$  levels?  $\text{Ca}^{2+}$  levels rise massively when parasites exit host cells and are required to activate motility. Perhaps linking amylopectin regulation to  $\text{Ca}^{2+}$  allows rapid mobilization of energy stores when parasites become extracellular so as to support the high levels of ATP that are likely required for motility.

Bradyzoites are thought to enter a metabolically quiescent state as they differentiate, decreasing glucose utilization and up-regulating the synthesis of amylopectin (or downregulating its breakdown). Amylopectin is therefore likely to be an important long-term energy store during chronic infection. Indeed, while loss of CDPK2 activity, and accompanying starch accumulation, appears to have relatively minor effects on tachyzoite growth both in cell culture and during infection, the effect on bradyzoites is much more severe. What is not clear is why bradyzoites seem to be so much more sensitive to amylopectin levels. It could potentially be that bradyzoite metabolism is already skewed to make more amylopectin than tachyzoites and that loss of CDPK2 exacerbates this. Another possibility is that bradyzoites are unable to dispose of excess amylopectin in the same way as tachyzoites. Unlike tachyzoites, bradyzoites do not appear to form a residual body, thus excess amylopectin cannot be removed from the parasite cell. Amylopectin therefore accumulates in the bradyzoite, physically disrupting and ultimately killing it. This would completely abrogate chronic *Toxoplasma* infection.

We show that the enzymatic activity of CDPK2 is required for its function and furthermore identify potential substrates of this kinase. Our work therefore suggests that the balance between amylopectin synthesis and degradation is likely regulated by protein phosphorylation by CDPK2. Indeed, in muscle and liver cells, protein phosphorylation is a regulatory mechanism of enzymes involved in the synthesis and degradation of glycogen (Roach et al., 2010). Our work also identifies these proteins as enzymes that are known to be involved in starch breakdown and synthesis in other systems and shows that these proteins can bind to sugar polymers and co-localize with CDPK2. What now appears to be important to understand is the functional role of these enzymes in amylopectin production and whether phosphorylation controls their activity. While we have shown that one of the identified proteins—GP, a protein predicted to be involved in starch breakdown—is also required for amylopectin homeostasis in *Toxoplasma*, we have yet to be able to show a role of individual phosphorylation sites in regulating the activity of this protein using the simple morphological readout. Clearly, to answer this question more thoroughly, more sensitive methods will need to be applied such as  $^{13}\text{C}$ -glucose tracer experiments, developing *in vitro* assays for the individual enzymes and generating compound phosphosite mutant parasites.

There are currently no therapeutic options to treat the 30%–80% of individuals chronically infected with *Toxoplasma*. Treatment options for latent infections would significantly benefit immunocompromised patients. Furthermore, if correlative links between chronic *Toxoplasma* infection and mental health conditions become stronger, then clearing chronic bradyzoite infections may also help treatment of some psychiatric disorders. We have shown that the loss of CDPK2 causes unchecked

production of amylopectin in *Toxoplasma* parasites, which results in non-viable bradyzoites and leads to a complete lack of cysts in the brain in a mouse model of infection. This strongly suggests that targeting this kinase (and/or one or more of its substrates) may be a viable therapeutic option for the treatment of chronic toxoplasmosis. Our work shows that CDPK2 is vital for bradyzoite development and for the establishment of chronic infection. The next important step will be to determine if it is required for the persistence of established cysts.

## EXPERIMENTAL PROCEDURES

### Parasite Culture, Transfection, and DNA Cloning

*Toxoplasma* tachyzoites were maintained in continuous culture and transfected as previously described (McCoy et al., 2012) (details in *Supplemental Experimental Procedures*). Differentiation of tachyzoites into bradyzoites and competition assays were performed as previously described (Nebi et al., 2011; Fox et al., 2011). DNA cloning was performed using primers and standard techniques outlined in *Supplemental Experimental Procedures*.

### Microscopy and Cellular Assays

Light microscopy of immuno-decorated samples was performed using standard procedures and captured on a Zeiss system equipped Axiovision software or a Deltavision Elite and SoftWoRx software. Detailed procedures along with methods for PAS staining and transmission electron microscopy can be found in *Supplemental Experimental Procedures*.

### Amylose Binding Assay

Approximately  $5 \times 10^8$  tachyzoites were resuspended in 500  $\mu\text{l}$  of lysis buffer (PBS containing 0.5% NP-40, 1 mM MgCl<sub>2</sub>, 25 U/ml Benzonase [Novagen], and protease and phosphatase inhibitors [Roche]). The lysates were incubated on ice for 30 min, before centrifuging at 17,000  $\times g$  for 10 min at 4°C.

The supernatants were mixed with 80  $\mu\text{l}$  of amylose beads (NEB) for 3 hr at 4°C. Unbound fractions were collected, and beads were washed five times with 400  $\mu\text{l}$  of PBS/0.2% NP-40, before resuspending in 40  $\mu\text{l}$  of SDS-PAGE sample buffer (Invitrogen). Amylose-bound proteins were eluted by heating at 95°C for 8 min. Proteins were resolved by SDS-PAGE followed by western blotting.

### Amylopectin Characterization and Quantification

Parasites were boiled in water for 10 min, and soluble material was incubated in 50 mM acetate buffer at pH 3.8 with or without 200 U isoamylase (Sigma) at 45°C, overnight. Reactions were heat inactivated, and the supernatants were desalted and run on a HPAEC (Dionex) equipped with amperometric detection. For amylopectin quantification, hot water extracts of freshly egressed filtered tachyzoites or scraped bradyzoite-infected and uninfected monolayers were resuspended in water, sonicated, and boiled for 10 min. The supernatant was digested by  $\alpha$ -glucosidase (Megazymes) in 0.1 M potassium buffer, pH 6.8, for 2 hr at 60°C. High-speed supernatants of heat-inactivated reactions were desalted, methanol washed, resuspended in 20  $\mu\text{l}$  pyridine, and trimethylsilylated in N,O-bis(trimethylsilyl)trifluoroacetamide (BSTFA-1% TMS) for 1 hr at room temperature. Glucose was analyzed by GC/MS on a DB-5MS + DG column (J&W, Agilent, 30 m  $\times$  0.25 mm, with 10 gap) equipped Agilent 7890A-5975C GC/MS. Chromatograms were processed in MSD Chemstation D.01.02.16 software (Agilent). Glucose background was estimated from undigested control samples and subtracted.

Stable isotope labeling, metabolite extraction, and analysis were carried out as described previously (MacRae et al., 2012, CHM) and are detailed in the *Supplemental Experimental Procedures*.

### Quantitative Proteomics and Substrate Capture by Thiophosphorylation

These protocols were essentially performed as previously published (Lourido et al., 2013; Nebi et al., 2011) with modifications and details that are outlined in *Supplemental Experimental Procedures*.

### Mouse Infections

8- to 12-week-old C57BL/6 male mice were injected intraperitoneally with 10,000 tachyzoites in 200  $\mu\text{l}$  of serum-free DME, carried out in accordance with the guidelines of the Walter and Eliza Hall Institute Animal Ethics Committee. Mice were sacrificed, and parasites were recovered by either intraperitoneal lavage with PBS with EDTA for tachyzoites or by brain tissue homogenization for cysts. Tachyzoites and bradyzoites were counted using either light or fluorescence microscopy.

## SUPPLEMENTAL INFORMATION

Supplemental Information includes seven figures, two tables, and Supplemental Experimental Procedures and can be found with this article online at <http://dx.doi.org/10.1016/j.chom.2015.11.004>.

## AUTHOR CONTRIBUTIONS

J.M.M. and A.D.U. conceived and performed experiments, provided parasite samples for co-authors, and wrote the manuscript. C.J.T. conceived experiments, wrote the manuscript, and secured funding. M.B. and M.J.M. performed metabolomic work. M.G. and S.L.M. conceived and performed mouse work. D.J.P.F. performed electron microscopy. L.F.D. and A.I.W. assisted with conception and performed SILAC-based proteomics. C.T.B. and A.B. performed methylation linkage analysis. D.I.S. and P.R.G. performed sequence alignment and protein modeling.

## ACKNOWLEDGMENTS

We would like to thank the following people for the kind donation of antibodies: J. Boothroyd, Stanford University (SRS9 and SAG1) and C. Beckers, University of North Carolina (GAP45). We would also like to thank Liana Mackiewicz from WEHI Bioservices, the WEHI Histology Department and Kelly Rogers, Lachlan Whitehead and Mark Scott from WEHI's Centre for Dynamic Imaging for expert help.

J.M.M. is supported by an Australian Postgraduate Award. C.T.B. and A.B. acknowledge the support of the ARC Centre of Excellence in Plant Cell Walls. This work was supported by Australian NHMRC project grant (GNT1022559) and an ARC/NHMRC Future Fellowship awarded to C.J.T. S.L.M. is the recipient of an NHMRC Career Development Fellowship and VESKI Fellowship, and M.J.M. is a NHMRC Principle Research Fellow. This work was also made possible through Victorian State Government Operational Infrastructure Support and Australian Government NHMRC IRISS. The funders had no role in study design, data collection, and analysis; decision to publish; or preparation of the manuscript.

Received: November 11, 2014

Revised: August 10, 2015

Accepted: November 13, 2015

Published: December 9, 2015

## REFERENCES

- Allen, J.J., Li, M., Brinkworth, C.S., Paulson, J.L., Wang, D., Hübner, A., Chou, W.H., Davis, R.J., Burlingame, A.L., Messing, R.O., et al. (2007). A semisynthetic epitope for kinase substrates. *Nat. Methods* 4, 511–516, <http://dx.doi.org/10.1038/nmeth1048>.
- Behnke, M.S., Fentress, S.J., Mashayekhi, M., Li, L.X., Taylor, G.A., and Sibley, L.D. (2012). The polymorphic pseudokinase ROP5 controls virulence in *Toxoplasma gondii* by regulating the active kinase ROP18. *PLoS Pathog.* 8, e1002992, <http://dx.doi.org/10.1371/journal.ppat.1002992>.
- Billker, O., Dechamps, S., Tewari, R., Wenig, G., Franke-Fayard, B., and Brinkmann, V. (2004). Calcium and a calcium-dependent protein kinase regulate gamete formation and mosquito transmission in a malaria parasite. *Cell* 117, 503–514.
- Billker, O., Lourido, S., and Sibley, L.D. (2009). Calcium-dependent signaling and kinases in apicomplexan parasites. *Cell Host Microbe* 5, 612–622, <http://dx.doi.org/10.1016/j.chom.2009.05.017>.

- Bishop, A.C., Ubersax, J.A., Petsch, D.T., Matheos, D.P., Gray, N.S., Blelloch, J., Shimizu, E., Tsien, J.Z., Schultz, P.G., Rose, M.D., et al. (2000). A chemical switch for inhibitor-sensitive alleles of any protein kinase. *Nature* 407, 395–401, <http://dx.doi.org/10.1038/35030148>.
- Blelloch, J.D., Glavy, J.S., Morgan, D.O., and Shokat, K.M. (2008). Covalent capture of kinase-specific phosphopeptides reveals Cdk1-cyclin B substrates. *Proc. Natl. Acad. Sci. USA* 105, 1442–1447, <http://dx.doi.org/10.1073/pnas.0708966105>.
- Blume, M., Rodriguez-Contreras, D., Landfear, S., Fleige, T., Soldati-Favre, D., Lucius, R., and Gupta, N. (2009). Host-derived glucose and its transporter in the obligate intracellular pathogen *Toxoplasma gondii* are dispensable by glutaminolysis. *Proc. Natl. Acad. Sci. USA* 106, 12998–13003, <http://dx.doi.org/10.1073/pnas.0903831106>.
- Carruthers, V.B., and Sibley, L.D. (1999). Mobilization of intracellular calcium stimulates microneme discharge in *Toxoplasma gondii*. *Mol. Microbiol.* 31, 421–428.
- Coppin, A., Dzierszinski, F., Legrand, S., Mortuaire, M., Ferguson, D., and Tomavo, S. (2003). Developmentally regulated biosynthesis of carbohydrate and storage polysaccharide during differentiation and tissue cyst formation in *Toxoplasma gondii*. *Biochimie* 85, 353–361, [http://dx.doi.org/10.1016/S0300-9084\(03\)00076-2](http://dx.doi.org/10.1016/S0300-9084(03)00076-2).
- Ferguson, D.J.P., and Hutchison, W.M. (1987). An ultrastructural study of the early development and tissue cyst formation of *Toxoplasma gondii* in the brains of mice. *Parasitol. Res.* 73, 483–491.
- Ferguson, D.J.P., Hutchison, W.M., Dunachie, J.F., and Slim, J.C. (1974). Ultrastructural study of early stages of asexual multiplication and microgametogony of *Toxoplasma gondii* in the small intestine of the cat. *Acta. Pathol. Microbiol. Scand. B Microbiol. Immunol.* 82, 167–181.
- Fleckenstein, M.C., Reese, M.L., Könen-Waisman, S., Boothroyd, J.C., Howard, J.C., and Steinfeldt, T. (2012). A *Toxoplasma gondii* pseudokinase inhibits host IRG resistance proteins. *PLoS Biol.* 10, e1001358, <http://dx.doi.org/10.1371/journal.pbio.1001358>.
- Fox, B.A., Falla, A., Rommereim, L.M., Tomita, T., Gigley, J.P., Mercier, C., Cesbron-Delaunay, M.-F., Weiss, L.M., and Bzik, D.J. (2011). Type II *Toxoplasma gondii* KU80 knockout strains enable functional analysis of genes required for cyst development and latent infection. *Eukaryot. Cell* 10, 1193–1206, <http://dx.doi.org/10.1128/EC.00297-10>.
- Gajria, B., Bahl, A., Brestell, J., Dommer, J., Fischer, S., Gao, X., Heiges, M., Iodice, J., Kissinger, J.C., Mackey, A.J., et al. (2008). ToxoDB: an integrated *Toxoplasma gondii* database resource. *Nucleic Acids Res.* 36, D553–D556, <http://dx.doi.org/10.1093/nar/gkm981>.
- Garrison, E., Treeck, M., Ehret, E., Butz, H., Garbuz, T., Oswald, B.P., Settles, M., Boothroyd, J., and Arrizabalaga, G. (2012). A forward genetic screen reveals that calcium-dependent protein kinase 3 regulates egress in *Toxoplasma*. *PLoS Pathog.* 8, e1003049, <http://dx.doi.org/10.1371/journal.ppat.1003049>.
- Glasner, P.D., Silveira, C., Kruszon-Moran, D., Martins, M.C., Burnier Júnior, M., Silveira, S., Camargo, M.E., Nussenblatt, R.B., Kaslow, R.A., and Belfort Júnior, R. (1992). An unusually high prevalence of ocular toxoplasmosis in southern Brazil. *Am. J. Ophthalmol.* 114, 136–144.
- Guérardel, Y., Leleu, D., Coppin, A., Liénard, L., Slomianny, C., Strecker, G., Ball, S., and Tomavo, S. (2005). Amylopectin biogenesis and characterization in the protozoan parasite *Toxoplasma gondii*, the intracellular development of which is restricted in the HepG2 cell line. *Microbes Infect.* 7, 41–48, <http://dx.doi.org/10.1016/j.micinf.2004.09.007>.
- Hill, D.E., Chirukandoth, S., and Dubey, J.P. (2005). Biology and epidemiology of *Toxoplasma gondii* in man and animals. *Anim. Health Res. Rev.* 6, 41–61.
- Huynh, M.-H., and Carruthers, V.B. (2009). Tagging of endogenous genes in a *Toxoplasma gondii* strain lacking Ku80. *Eukaryot. Cell* 8, 530–539, <http://dx.doi.org/10.1128/EC.00358-08>.
- Lourido, S., Shuman, J., Zhang, C., Shokat, K.M., Hui, R., and Sibley, L.D. (2010). Calcium-dependent protein kinase 1 is an essential regulator of exocytosis in *Toxoplasma*. *Nature* 465, 359–362, <http://dx.doi.org/10.1038/nature09022>.
- Lourido, S., Tang, K., and Sibley, L.D. (2012). Distinct signalling pathways control *Toxoplasma* egress and host-cell invasion. *EMBO J.* 31, 4524–4534, <http://dx.doi.org/10.1038/emboj.2012.299>.
- Lourido, S., Jeschke, G.R., Turk, B.E., and Sibley, L.D. (2013). Exploiting the unique ATP-binding pocket of *Toxoplasma* calcium-dependent protein kinase 1 to identify its substrates. *ACS Chem. Biol.* 8, 1155–1162, <http://dx.doi.org/10.1021/cb400115y>.
- MacRae, J.I., Sheiner, L., Nahid, A., Tonkin, C., Striepen, B., and McConville, M.J. (2012). Mitochondrial metabolism of glucose and glutamine is required for intracellular growth of *Toxoplasma gondii*. *Cell Host Microbe* 12, 682–692, <http://dx.doi.org/10.1016/j.chom.2012.09.013>.
- McCoy, J.M., Whitehead, L., van Dooren, G.G., and Tonkin, C.J. (2012). TgCDPK3 regulates calcium-dependent egress of *Toxoplasma gondii* from host cells. *PLoS Pathog.* 8, e1003066, <http://dx.doi.org/10.1371/journal.ppat.1003066>.
- Morlon-Guyot, J., Berry, L., Chen, C.-T., Gubbels, M.-J., Lebrun, M., and Daher, W. (2013). The *Toxoplasma gondii* calcium-dependent protein kinase 7 is involved in early steps of parasite division and is crucial for parasite survival. *Cell Microbiol.* 16, 95–114.
- Nebl, T., Prieto, J.H., Kapp, E., Smith, B.J., Williams, M.J., Yates, J.R., 3rd, Cowman, A.F., and Tonkin, C.J. (2011). Quantitative in vivo analyses reveal calcium-dependent phosphorylation sites and identifies a novel component of the *Toxoplasma* invasion motor complex. *PLoS Pathog.* 7, e1002222, <http://dx.doi.org/10.1371/journal.ppat.1002222>.
- Oppenheim, R.D., Creek, D.J., Macrae, J.I., Modrzynska, K.K., Pino, P., Limenitakis, J., Polonais, V., Seeber, F., Barrett, M.P., Billker, O., et al. (2014). BCKDH: the missing link in apicomplexan mitochondrial metabolism is required for full virulence of *Toxoplasma gondii* and *Plasmodium berghei*. *PLoS Pathog.* 10, e1004263, <http://dx.doi.org/10.1371/journal.ppat.1004263>.
- Pettolino, F.A., Walsh, C., Fincher, G.B., and Bacic, A. (2012). Determining the polysaccharide composition of plant cell walls. *Nat. Protoc.* 7, 1590–1607, <http://dx.doi.org/10.1038/nprot.2012.081>.
- Roach, P.J., Skurat, A.V., and Harris, R.A. (2010). Regulation of Glycogen Metabolism (John Wiley & Sons, Inc.). <http://dx.doi.org/10.1002/cphy.cp070219>.
- Sebastian, S., Brochet, M., Collins, M.O., Schwach, F., Jones, M.L., Goulding, D., Rayner, J.C., Choudhary, J.S., and Billker, O. (2012). A *Plasmodium* calcium-dependent protein kinase controls zygote development and transmission by translationally activating repressed mRNAs. *Cell Host Microbe* 12, 9–19, <http://dx.doi.org/10.1016/j.chom.2012.05.014>.
- Siden-Kiamos, I., Ecker, A., Nybäck, S., Louis, C., Sinden, R.E., and Billker, O. (2006). *Plasmodium berghei* calcium-dependent protein kinase 3 is required for ookinete gliding motility and mosquito midgut invasion. *Mol. Microbiol.* 60, 1355–1363, <http://dx.doi.org/10.1111/j.1365-2958.2006.05666.x>.
- Torgerson, P.R., and Mastroiacovo, P. (2013). The global burden of congenital toxoplasmosis: a systematic review. *Bull. World Health Organ.* 91, 501–508, <http://dx.doi.org/10.2471/BLT.12.111732>.
- Wernimont, A.K., Artz, J.D., Finerty, P., Jr., Lin, Y.-H., Amani, M., Allali-Hassani, A., Senisterra, G., Vedadi, M., Tempel, W., Mackenzie, F., et al. (2010). Structures of apicomplexan calcium-dependent protein kinases reveal mechanism of activation by calcium. *Nat. Struct. Mol. Biol.* 17, 596–601, <http://dx.doi.org/10.1038/nsmb.1795>.